PAPER • OPEN ACCESS

First assessment on suspension parameter optimization for a solar – powered vehicle

View the article online for updates and enhancements.

First assessment on suspension parameter optimization for a solar – powered vehicle

S Sorrentino[1], A De Felice[1], P Grosso[1] and G Minak[2]

[1]University of Modena and Reggio Emilia, Department of Engineering Enzo Ferrari, Via Vivarelli 10, 41125 Modena, Italy
[2]University of Bologna, Department of Industrial Engineering, Viale Risorgimento 2, 40136, Bologna, Italy

E-mail: pasquale.grosso@unimore.it

Abstract. Optimization of suspension parameters with respect to comfort and road holding is a challenging issue for solar–powered cars, due to in–wheel electric engines on very light vehicles, carrying payloads which can exceed their total mass. The solar–powered car considered in this study was designed and manufactured for racing by the University of Bologna; with a mass of 300 kg and a payload of 320 kg due to four occupants, using 5 m^2 of monocrystalline silicon photovoltaic panel on the roof, 64 kg of lithium–ion batteries and two electric engines coupled directly to the rear wheels, it can achieve either a range of 600 km at cruising speed, or velocity peaks of 120 km/h. In this contribution, equivalent vertical stiffness and equivalent damping coefficients are optimized for both axles, achieving results that in terms of comfort and road holding are comparable to those of standard passenger cars.

1. Introduction

The interest in solar–powered vehicles arose as a topic of study mainly developed by academic institutions [1,2] with the aim of promoting sustainable mobility [3], including new standards and regulations [4]. The main challenges in designing such cutting–edge vehicles [5,6] consist in electrical systems, solar array design, structural materials [7] and mechanical subsystems such as suspensions [8]. Focusing on suspension systems, the load due to passengers, electric batteries and solar panels can be even higher than the total weight of the remaining parts of the vehicle, making the choice of suspension stiffness and weight distribution quite challenging in order to get good performances in terms of vehicle dynamics [9,10]. These technical demands become extreme in the case of the so-called 'cruiser' category, i.e. multi–passenger vehicles recently introduced in solar–powered car competitions. In fact, compared to more traditional single–seater solar cars, cruisers present a total weight from four to five times higher, as well as higher center of gravity [11].

The solar–powered car considered in this study and displayed in Figure 1 was designed and manufactured for racing. It is equipped with a solar–electric powertrain developed for efficiently transporting four passengers weighing 80 kg each. With a monocoque, structural and non–structural parts in carbon fiber reinforced polymer (CFRP), a roll–cage in titanium alloy among other distinct technical features, it represents one of the lightest multi–occupant solar cars ever built: a vehicle with total mass of 320 kg allows to transport 320 kg due to four occupants. Using 5 m^2 of monocrystalline silicon photovoltaic panel on the roof, 64 kg of lithium–ion batteries, two electric engines coupled directly to the rear wheels and further solutions for optimal energy control, either a range of 600 km at cruising speed, or velocity peaks of 120 km/h can be achieved [11].
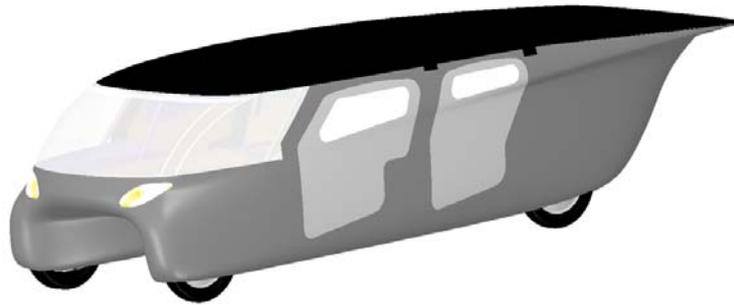
Figure 1. Solar–powered car under investigation [11].

However, this vehicle still needs further mechanical improvements, for increasing the average speed of the race vehicle up to 75 km/h, a necessary condition to successfully take part in further competitions. In particular, the current suspension system (as shown in Figure 2) has to be designed considering the necessity to provide adequate levels of handling, road holding, comfort and vibration control in a process of design review and optimisation as done for more conventional vehicles [12,13].
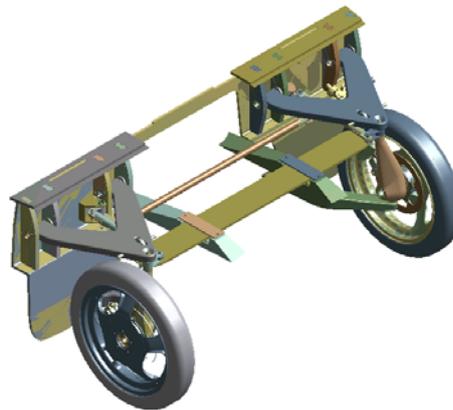
Figure 2. Suspension system under investigation [11].

The focus of the present contribution is a first assessment on optimization of the main parameters affecting comfort and road holding, which are the equivalent stiffness and damping of the suspensions [14] for this multi-occupant solar–powered car.

To this purpose, in section 2 the equivalent vertical stiffness of the front and rear axles are tuned in order to fit the basic requirements for comfort in terms of natural frequencies and mode shapes of bounce and pitch [15]; the optimization of suspension damping [16] is then addressed in section 3, for reaching a good compromise between comfort and road holding, aimed at achieving results comparable to those of standard passenger cars.

2. Tuning of suspension stiffness

Two fundamental parameters in car suspension design are first considered, the dynamic index r_1 (related to mass distribution) and the stiffness index r_2 (related to the equivalent vertical stiffness of the two axles) [14], which are defined by:

$$r_1 = \frac{J_y}{m_s a_1 a_2}, \quad r_2 = \frac{k_1 a_1}{k_2 a_2} \tag{1}$$

where m_s is the total sprung mass, J_y is the lateral moment of inertia with respect to the center of gravity, a_1 and a_2 are the front and rear partial wheelbases (longitudinal distances of the center of gravity from the front and rear axles respectively, where $a_1 + a_2 = l$ is the wheelbase), while k_1 and k_2

are the equivalent vertical stiffness of the front and rear axles, respectively. Usually in road cars r_1 ranges between 0.90 and 0.97, while r_2 is set between 0.90 and 0.95 for respecting current standards in suspension design [14]. A 2–dofs model for free vertical oscillations is adopted, according to:

$$\mathbf{M\ddot{s} + Ks = 0}, \quad \mathbf{M} = \begin{bmatrix} m_s & 0 \\ 0 & J_y \end{bmatrix}, \quad \mathbf{K} = \begin{bmatrix} K_{11} & K_{12} \\ K_{21} & K_{22} \end{bmatrix} = \begin{bmatrix} k_1 + k_2 & k_1 a_1 - k_2 a_2 \\ k_1 a_1 - k_2 a_2 & k_1 a_1^2 + k_2 a_2^2 \end{bmatrix}, \quad \mathbf{s} = \begin{Bmatrix} z_G \\ \vartheta \end{Bmatrix} \tag{2}$$

where z_G is the vertical displacement of the center of gravity of the sprung mass and ϑ is the pitch angle, yielding the natural angular frequencies of the so–called bounce and pitch modes as:

$$\omega_{1,2} = \sqrt{\frac{m_s K_{22} + J_y K_{11} \mp \sqrt{(m_s K_{22} - J_y K_{11})^2 + 4 m_s J_y K_{12} K_{21}}}{2 m_s J_y}} \tag{3}$$

while the nodes of the two mode shapes are given by the following longitudinal coordinates (positive values backwards with respect to the center of gravity):

$$x_{01} = \frac{\omega_1^2 J_y - K_{22}}{K_{21}}, \quad x_{02} = \frac{\omega_2^2 J_y - K_{22}}{K_{21}} \tag{4}$$

Assuming at a first stage $r_1 = 1$, then the nodes in equations (4) are located on the vertical of the two axles; moreover, if $r_2 < 1$ then the two natural angular frequencies are simply given by:

$$\omega_1 = \sqrt{\frac{k_1 l}{m_s (l - a_1)}} = \sqrt{\frac{g}{\Delta z_1}}, \quad \omega_2 = \frac{1}{\sqrt{r_2}} \omega_1 > \omega_1, \quad \Delta z_2 = r_2 \Delta z_1 < \Delta z_1 \tag{5}$$

where Δz_1 and Δz_2 are the static deflections at the front and rear axles, respectively. An upper bound for the largest static deflection produces a lower bound for the first natural frequency.
Setting $r_2 = 0.95$ and $\Delta z_1 = 150$ mm (design upper limit for the car under study) yields $\Delta z_2 = 142.5$ mm, $f_1 = 1.29$ Hz, $f_2 = 1.32$ Hz. The effect of reducing r_2 would simply be that of reducing Δz_2 and increasing f_2, according to equations (5). The (realistic) effect of reducing r_1 is addressed in section 4.

3. Tuning of suspension damping
The damping distribution is set to give a damping matrix proportional to the stiffness matrix in equations (2), i.e. $\mathbf{C} = \beta \mathbf{K}$, with damping coefficients $c_1 = \beta k_1$ and $c_2 = \beta k_2$ (as a consequence, the mode shapes are the same of the related undamped model).
For selection of the damping coefficients c, a different 2–dofs model is adopted, usually called Quarter car model, but herein referred to forced vibration of the whole vehicle [6], according to:

$$\mathbf{M\ddot{x} + C\dot{x} + Kx = f}, \quad \mathbf{M} = \begin{bmatrix} m_s & 0 \\ 0 & m_n \end{bmatrix}, \quad \mathbf{C} = \begin{bmatrix} c & -c \\ -c & c \end{bmatrix}, \quad \mathbf{K} = \begin{bmatrix} k & -k \\ -k & k+p \end{bmatrix}, \quad \mathbf{f} = \begin{Bmatrix} 0 \\ ph \end{Bmatrix}, \quad \mathbf{x} = \begin{Bmatrix} z \\ y \end{Bmatrix} \tag{6}$$

where m_n is the total unsprung mass, $c = \beta k$, $k = k_1 + k_2$ (hence $c_1 = \beta k_1$, $c_2 = \beta k_2$), p is the total vertical stiffness of the tyres, h is the displacement imposed at the ground by uneven surface (assumed harmonic, with angular frequency ω), z and y are the displacements of m_s and m_n, respectively. Notice that in this model the longitudinal position of the center of gravity, and therefore a_1, a_2, are not influential. The two natural frequencies of the undamped model described by equations (6) are:

$$\omega_{1,2}^{(i)} = \frac{1}{2} \left[\frac{p+k}{m_n} + \frac{k}{m_s} \mp \sqrt{\left(\frac{p+k}{m_n} - \frac{k}{m_s} \right)^2 + \frac{4k^2}{m_n m_s}} \right] \tag{7}$$

According to the following data (design parameters for the car under study): $m_s = 584$ kg, $m_n = 59.32$ kg, $k = 39203$ N/m (due to $r_1 = r_2 = 0.95$, $a_1 = 1421$ mm, $k_1 = 18748$ N/m, $k_2 = 20455$ N/m), $p = 3.6 \times 10^5$ N/m, then equation (7) yields $f_1 = 1.24$ Hz, $f_2 = 13.06$ Hz (with $f_2 / f_1 \approx 10$, a typical value for road cars). As suggested by Bourcier de Carbon [16], a choice for an 'optimal' damping coefficient c is:

$$c_o = \sqrt{\frac{m_s k}{2}} \sqrt{\frac{p + 2k}{p}} \tag{8}$$

in this case yielding c_o = 3734 Ns/m (which, introducing $\mathbf{C} = \beta\mathbf{K}$ in equations 2, gives modal damping ratios in the usual range of 0.38 to 0.40).

Equation (8) provides a value close to what can be considered the best choice for coefficient c in terms of comfort optimization, which has to be increased for road holding optimization [14]. To this purpose the following frequency response functions are considered:

1) receptance R_Z between amplitude Z (m_s vertical displacement) and amplitude H of ground harmonic input ($\omega^2 R_Z$ yielding a measure of m_s vertical acceleration, to be minimized for comfort optimization):

$$R_Z = \frac{|Z|}{H} = p\sqrt{\frac{k^2 + c^2\omega^2}{h_1^2(\omega) + c^2\omega^2 h_2^2(\omega)}}, \quad \begin{cases} h_1(\omega) = m_s m_n \omega^4 - \left[(p+k)m_s + k m_n\right]\omega^2 + pk \\ h_2(\omega) = p - (m_s + m_n)\omega^2 \end{cases} \tag{9}$$

2) receptance R_Y between amplitude Y (m_n vertical displacement), and amplitude H:

$$R_Y = \frac{|Y|}{H} = p\sqrt{\frac{(k - m_s\omega^2)^2 + c^2\omega^2}{h_1^2(\omega) + c^2\omega^2 h_2^2(\omega)}} \tag{10}$$

3) receptance R_{Z-Y} between relative amplitude $Z - Y$, and amplitude H:

$$R_{Z-Y} = \frac{|Z - Y|}{H} = \frac{p\, m_s \omega^2}{\sqrt{h_1^2(\omega) + c^2\omega^2 h_2^2(\omega)}} \tag{11}$$

4) transmissibility T between ground vertical force amplitude N, and force pH:

$$T = \frac{N}{pH} = \omega^2 \sqrt{\frac{\left[m_s m_n \omega^2 - k(m_s + m_n)\right]^2 + c^2\omega^2(m_s + m_n)^2}{h_1^2(\omega) + c^2\omega^2 h_2^2(\omega)}} \tag{12}$$
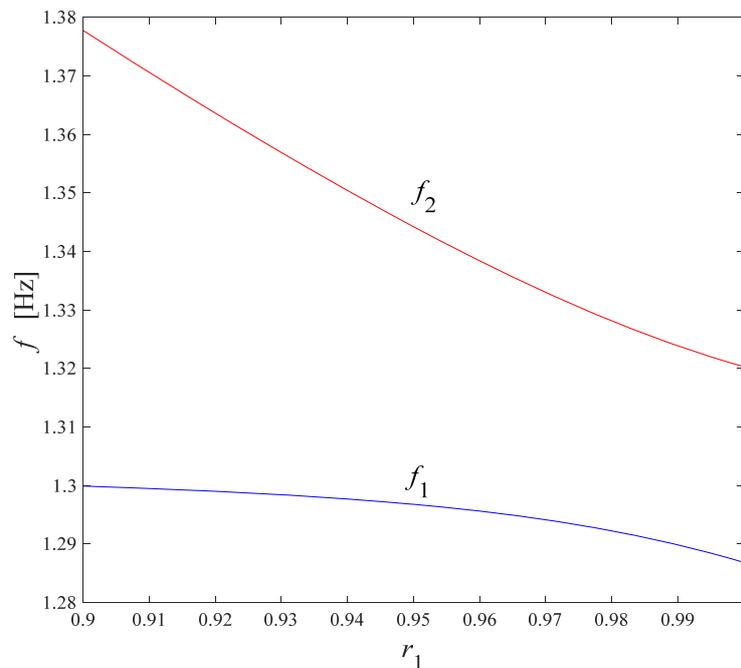
Figure 3. Effect of dynamic index r_1 (setting the stiffness index $r_2 = 0.95$) on natural frequencies of bounce (f_1) and pitch (f_2).
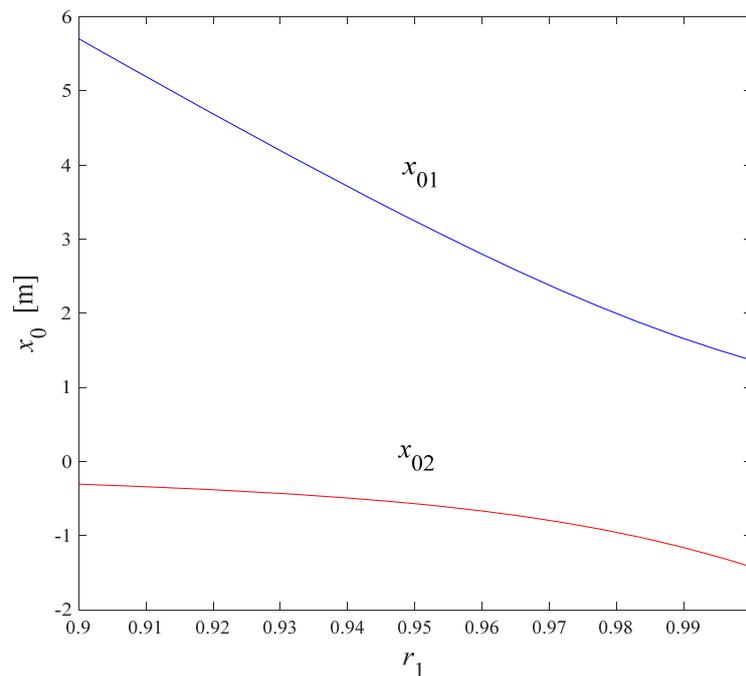
Figure 4. Effect of dynamic index r_1 (setting the stiffness index $r_2 = 0.95$) on the longitudinal position of nodes x_{01} (bounce mode) and x_{02} (pitch mode).

4. Results and discussion

The effects of reducing r_1 (from 1 to 0.9, for realistic mass distributions) can be studied by means of equations (2) to (4), with the following data (design parameters for the car under study): $m_s = 584$ kg, $l = 2792$ mm, $a_1 = 1421$ mm.

As shown in figures 3 and 4 for $r_2 = 0.95$, reducing r_1 from 1 to 0.9 produces a moderate increase of both natural frequencies (however without exceeding the upper bound of 1.50 Hz) together with a large shift of the nodal points x_{01} and x_{02} (x_{01} increases, meaning that the modal shape of the first mode, with lower natural frequency, is getting closer to that of pure bounce; while x_{02} reduces, meaning that the modal shape of the second mode, with higher natural frequency, is getting closer to that of pure pitch). Having the second nodal point (x_{02}) close to the center of gravity, and a bit ahead of it, helps to enhance the comfort of driver and passengers on front seats [6,7]. Realistic variations of a_1 do not affect significantly the results reported in figures 3 and 4 (1.0 Hz $< f_1 < f_2 <$ 1.5 Hz, mode at lower natural frequency f_1 = bounce, mode at higher natural frequency f_2 = pitch).

Therefore, with the adopted design parameters (mass distribution, partial wheelbases), it is possible in any case to fulfil the basic comfort requirements for free vibration, that is: 1) natural frequencies of bounce and pitch modes falling in the range 1.0 – 1.5 Hz; 2) pitch mode with its node located at about the front seats [15], as shown in figures 3 and 4. Slight variations of mass distribution (due to different arrangements of the battery pack) would result in small corrections to equivalent vertical stiffness parameters (in index r_2, equation 1), without affecting comfort.

Regarding forced vibration, in road cars the main interest is minimizing the amplitude of vertical acceleration of the sprung mass [14,16], for optimizing comfort.

As shown in Figure 5, c_o computed with equation (8) and $r_1 = r_2 = 0.95$ is a very good choice for improving comfort in the specific case of the car under study, since it yields a frequency response function with amplitudes comparable to those of standard passenger cars [14]. However, as shown in figure 6, for improving significantly road holding, c should be moderately increased (at least to $1.3c_o$), thus affecting comfort. Notice that increasing c would also have the advantageous effect of reducing the maximum amplitude of relative displacement between sprung and unsprung masses, as displayed in Figure 7.
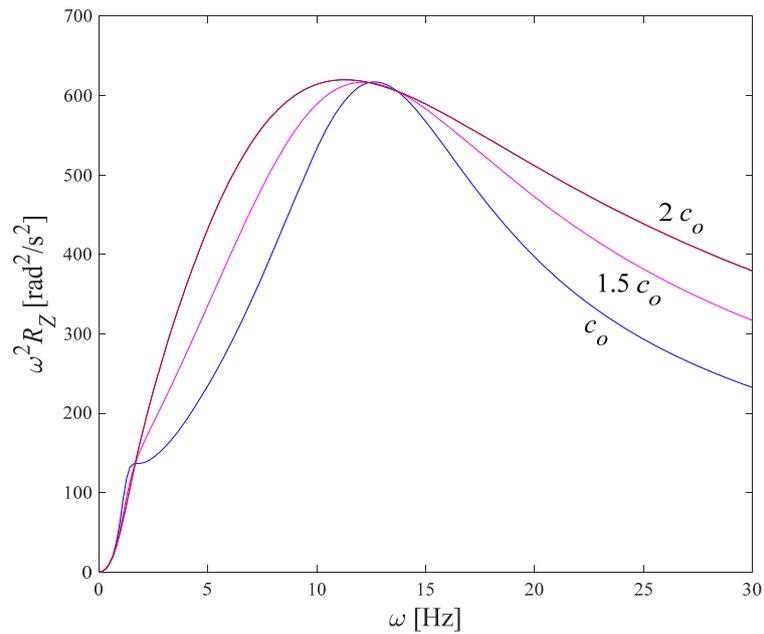
Figure 5. Amplification factor for the sprung mass m_s vertical acceleration ($\omega^2 R_Z$) as a function of frequency, for different values of suspension damping.
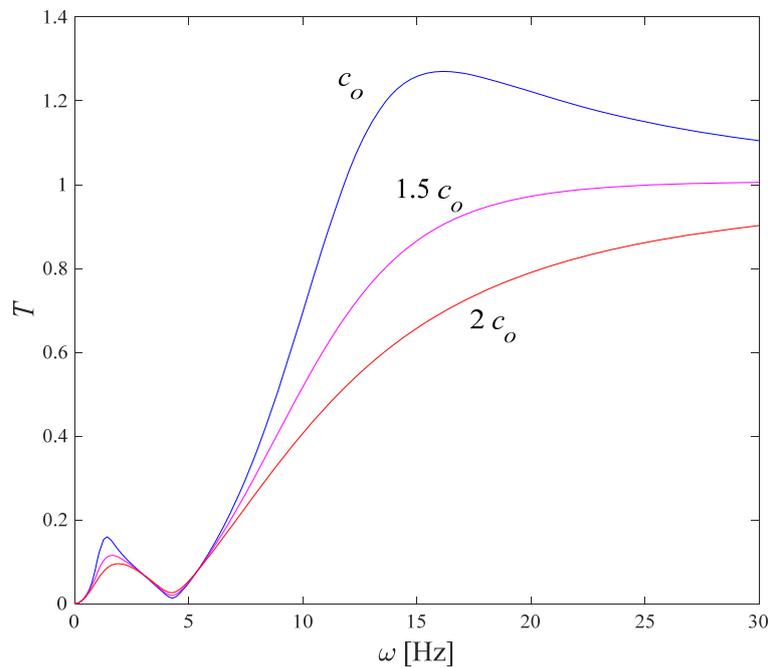
Figure 6. Transmissibility between ground vertical force amplitude N and force pH as a function of frequency (equation 12), for different values of suspension damping.
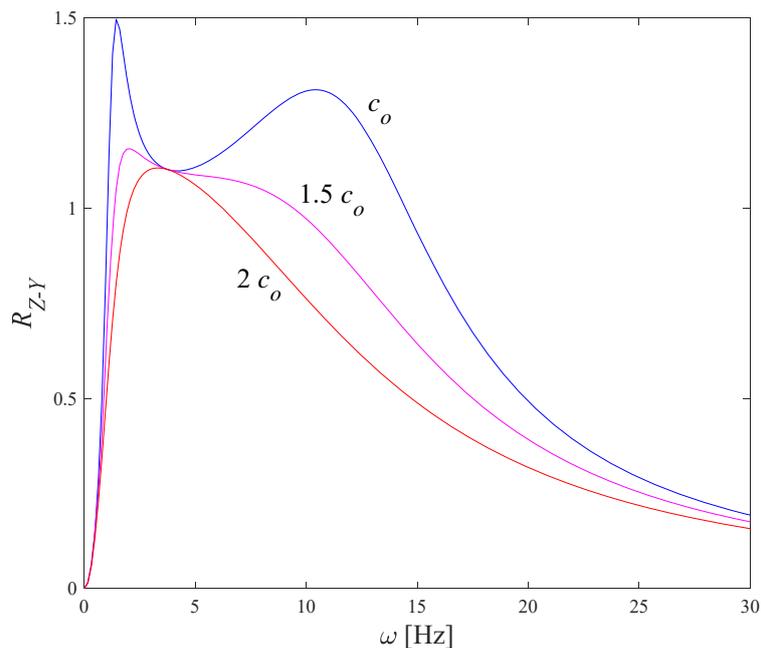
Figure 7. Amplification factor between relative amplitude $Z - Y$, and amplitude H as a function of frequency (equation 11), for different values of suspension damping.

5. Conclusions

In this contribution a preliminary study has been presented regarding the optimization of the suspension equivalent stiffness and damping parameters in the case of the Italian solar–powered multi-occupant car. This vehicle was designed and manufactured by the University of Bologna, together with the support of other Italian institutions, with the scope to compete in exclusive solar challenges all over the world. And it won in 2018 its first competition, the American Solar Challenge, running for 1,700km with 4 passengers and a cruising speed of, approximately, 65 km/h. But racing rules never stop to pretend more with the declared scope to foster researches and results on the solar mobility. Thus, an average speed higher than 75 km/h is now requested to take part to the next international competition, the World Solar Challenge, October 2019. This target also means a desired maximum speed of around 120-130km/h for an extremely light quadricycle. Nevertheless, this performance cannot be achieved without a relevant redesign and optimization in terms of vehicle dynamic, where this study represents a first fundamental step.

The equivalent vertical stiffness of the front and rear axles has been tuned in order to fit the basic requirements for comfort in terms of natural frequencies and mode shapes of bounce and pitch. The suspension damping has then been optimized for reaching a good compromise between comfort and road holding, aimed at achieving results comparable to those of standard passenger cars.

Acknowledgment

References

[1]   Wamborikar Y S and Sinha A *Solar powered vehicle*, World Congress on Engineering and Computer Science, October 2010, Vol. 2, pp. 20-22
[2]   Rizzo G, Arsie I and Sorrentino, M, *Solar energy for cars: perspectives, opportunities and problems*. In GTAA Meeting, 2010, May, pp. 1-6

[3]   Zacharof N, Fontaras G, Ciuffo B et al. 2016 *Review of in use factors affecting the fuel consumption and CO2 emissions of passenger cars*. European Union, EUR 27819 EN, doi:10.2790/140640

[4]   Pavlovic A and Fragassa C 2015 General considerations on regulations and safety requirements for quadricycles, *International Journal for Quality Research* **9**(4) 657-674

[5]   Fenton J and Hodkinson R 2001 *Lightweight electric/hybrid vehicle design*, Butterworth–Heinemann

[6]   Thacher E F 2015 *A Solar Car Primer: A Guide to the Design and Construction of Solar–Powered Racing Vehicles*, Springer

[7]   de Camargo F V, Fragassa C, Pavlovic A and Martignani M 2017 Analysis of the Suspension Design Evolution in Solar Cars, *FME Transactions* **45**(3) 394–404

[8]   Odabaşi V, Maglio S, Martini A and Sorrentino S 2019 Static Stress Analysis of Suspension Systems for a Solar–Powered Car, *FME Transactions* **47**(1) 70–75

[9]   Arsie I, Rizzo G and Sorrentino M 2006 Optimal design and dynamic simulation of a hybrid solar vehicle. *SAE Technical Paper* No. 2006-01-2997.

[10]   Minak G, Fragassa C and de Camargo F V 2017 *A brief review on determinant aspects in energy efficient solar car design and manufacturing*, International Conference on Sustainable Design and Manufacturing, Bologna, Italy, April 26 – 28, pp. 847-856

[11]   Minak G, Brugo T M, Fragassa C, Pavlovic A, de Camargo F V and Zavatta N 2019 Structural Design and Manufacturing of a Cruiser Class Solar Vehicle, *Journal of Visualized Experiments* **143** 1–15

[12]   Martini A, Bellani G and Fragassa C 2018 Numerical assessment of a new hydro-pneumatic suspension system for motorcycles, *International Journal of Automotive and Mechanical Engineering* **15**(2) 5308-5325

[13]   Leonelli L, Cattabriga S and Sorrentino S 2018 Driveline instability of racing motorcycles in straight braking manoeuvre, *Proceedings of the Institution of Mechanical Engineers, Part C: Journal of Mechanical Engineering Science* **232**(17) 3045-3061

[14]   Guiggiani M 2014 *The Science of Vehicle Dynamics*, Springer

[15]   Olley M 1934 Independent wheel suspension – its whys and wherefores, *SAE Transactions* **34**(3) 73–81

[16]   Bourcier de Carbon C 1950 *Theorie mathématique et réalisation pratique de la suspension amortie des véhicules terrestres*, Troisieme Congres Technique de l'Automobile, Paris, France